ChemComm

Accepted Manuscript

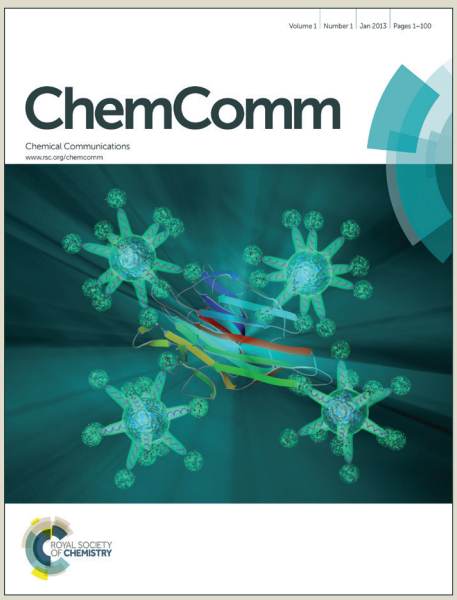

This is an *Accepted Manuscript*, which has been through the Royal Society of Chemistry peer review process and has been accepted for publication.

Accepted Manuscripts are published online shortly after acceptance, before technical editing, formatting and proof reading. Using this free service, authors can make their results available to the community, in citable form, before we publish the edited article. We will replace this *Accepted Manuscript* with the edited and formatted *Advance Article* as soon as it is available.

You can find more information about *Accepted Manuscripts* in the Information for Authors.

Please note that technical editing may introduce minor changes to the text and/or graphics, which may alter content. The journal's standard Terms & Conditions and the Ethical guidelines still apply. In no event shall the Royal Society of Chemistry be held responsible for any errors or omissions in this *Accepted Manuscript* or any consequences arising from the use of any information it contains.

ROYAL SOCIETY OF CHEMISTRY

www.rsc.org/chemcomm

Cite this: DOI: 10.1039/c0xx00000x

www.rsc.org/xxxxxx

ARTICLE TYPE

Octahedral-shaped perovskite nanocrystals and their visible-light photocatalytic activity†

Simin Yin,[a‡] He Tian,[b‡] Zhaohui Ren,*[a] Xiao Wei, [ac] Chunying Chao,[a] Jingyuan Pei,[ac] Xiang Li,[a] Gang Xu,[a] Ge Shen[a] and Gaorong Han*[a]

Received (in XXX, XXX) Xth XXXXXXXXX 20XX, Accepted Xth XXXXXXXXX 20XX

DOI: 10.1039/b000000x

Octahedral-shaped perovskite $PbTiO_3$ nanocrystals (PT OCT) with well-defined {111} facets exposed have been successfully synthesized via a facile hydrothermal method by using $LiNO_3$ as an ion surfactant. The Li-O bond on the surface of PT OCT nanocrystals is essential to the stability of such nanocrytals and also results in a dramatic high visible-light photocatalytic activity.

Solar-energy driven photocatalysis is a promising approach to treating water pollution and generating hydrogen.[1] Pioneered by Fujishima and Honda in 1972, TiO_2-based photocatalysts and photocatalytic activity have been the focus of much effort.[2] However, intrinsic photocatalysis of TiO_2 is limited to ultraviolet light (UV) due to a large band gap. Alternative ways, such as doping (B, C and N) and surface hydrogenation, have been proven to improve efficiency and to extend its response to visible light range by the way of modifying the optical band structure and absorption.[3] Stimulated by these researches, exploring new material systems for visible-light photocatalysis is of particular interest. As the well-known functional materials, perovskite and its derivative oxides have been widely explored as photocatalysts.[4] For instance, as typical perovskite oxides, $CaTiO_3$, $SrTiO_3$ and $BiFeO_3$ have been verified to present high UV photocatalytic activity, and in contrast to low visible one.[5] Analogous to intrinsic TiO_2, perovskite and related materials usually adopt a large band gap (>3.0 eV), which is out of visible light range. To achieve the photocatalytic activity of perovskite oxides under visible light, structure tailoring methods such as doping and heterogeneous composites with simple oxides and noble metals are popular strategies.[4,6] By taking the advantage of structure tailoring of perovskite oxides, we have an opportunity to design and prepare visible-light photocatalysts in a desirable way. Nevertheless, doping and heterogeneous composites for perovskite oxides usually require relatively complex process, high-temperature sintering for a long term and high cost for noble metals. Developing a facile method to synthesize high-performance visible-light perovskite photocatalysts remains an undergoing challenge.[7]

In this communication, we developed a facile hydrothermal method by using alkali metallic nitride ($LiNO_3$) as surfactant to synthesize octahedral-shaped nanocrystals of perovskite tetragonal $PbTiO_3$ (PT OCT) for the first time. With a size range of 50~100 nm and enclosed by {111} facets, PT OCT nanocrystals demonstrate a high activity in the degradation of methylene blue (MB) aqueous solution under visible light irradiation, and the first-order kinetic constant for the PT OCT nanocrystals was determined to be 0.042. Results from Electron Energy Loss Spectroscopy (EELS) and X-ray photoelectron spectroscopy (XPS) confirmed that the existence of Li-O bond on the surface would be strongly essential to the formation and stability of PT OCT nanocrystals that is critical to extend an optical absorption of PT to visible light range.

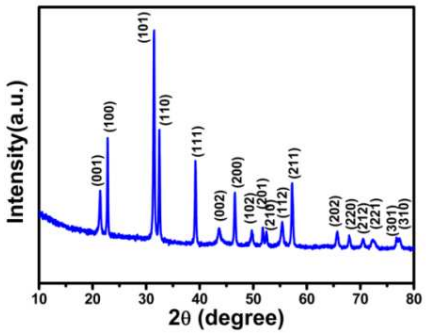

Fig. 1 Typical XRD pattern of the as-synthesized PT OCT nanocrystals.

Fig.1 presents the typical XRD pattern of the PT OCT nanocrystals synthesized under the optimal hydrothermal conditions (the detailed preparation procedure is described in Electroninic Supporting Information, ESI). It reveals that the as-synthesized PT OCT nanocrystals are highly crystallized, and all the diffraction peaks can be indexed into those of tetragonal perovskite PT phase (JCPDS file no. 06-0452), which is further confirmed by the Raman analysis (Fig. S1, ESI). In addition, a phase transformation temperature from perovskite ferroelectric tetragonal to paraelectric cubic one has been determined to be 485 ^oC, very close to the counterpart of a bulk[8] (Fig. S2). SEM image (Fig. S3) indicates that the sample consists of large-scale PT nanocrystals with regular facets, where Pb, Ti and O elements have been identified by corresponding energy dispersive spectroscopy (EDS). High magnitude SEM image in Fig. 2a clearly demonstrates that these PT nanocrystals actually adopt an octahedral shape, and the size of the nanocrystals ranges from 50-100 nm, matching well with the observations in low-magnification transmission electron microscopy (TEM) image of Fig. 2b. High-angle annular dark field scanning transmission electron microscopy (HADDF-STEM) has been employed to characterize the crystal fringes of a single PT OCT nanocrystal.

ChemComm Accepted Manuscript

The 0.285 nm and 0.227 nm interval of lattice fringes observed in Fig. 2c agrees well with the spacing of the (101) and (11-1) of tetragonal perovskite PT phase (JCPDS file no. 06-0452), respectively. Clear lattice image in the edge and inner part of the PT OCT combined with the above results, identifies that the as-synthesized PT OCT nanocrystals are single-crystal in character.

Combined SEM and STEM results, it is proposed that the PT OCT nanocrystal is probably enclosed by eight equal {111} facets. To further confirm such assumption, TEM images and corresponding selected area electron diffractions (SAED) of PT OCT nanocrystals along [001] and [111] zone axis were recorded, respectively, as shown in Fig. 2d-2g. Viewed along [001] orientation of single PT OCT nanocrystal, the projection presents a well-defined square (Fig. 2d), and corresponding SAED pattern (Fig. 2e) can be indexed into lattice spacing of (100) and (010) by tetragonal perovskite PT phase (JCPDS file No. 06-0452). The dark contrast dots in Fig. 2d correspond to Pb particles precipitating from the PT OCT nanocrystals due to electron beam irradiation. This implies that PT OCT nanocrystals present similar geometry configuration to that of TiO_6 octahedron in the unit cell of tetragonal perovskite PT. Therefore, the exposed facets of PT OCT nanocrystals can be confirmed as {111}. TEM image in Fig. 2f shows a regular hexagon shape for a single PT OCT nanocrystal, where the electron beam is perpendicular to the {111} facet, matching very well with that of In_2O_3 OCT enclosed by {111} facets.[9] The sharp diffraction spots in SAED pattern of Fig. 2g can be indexed into (10-1) and (1-10) of tetragonal perovskite PT. The results determined from Fig. 2 is furthermore supported by the projections of a simple OCT model, geometrically derived from {111} of tetragonal perovskite PT. (Fig. S4).

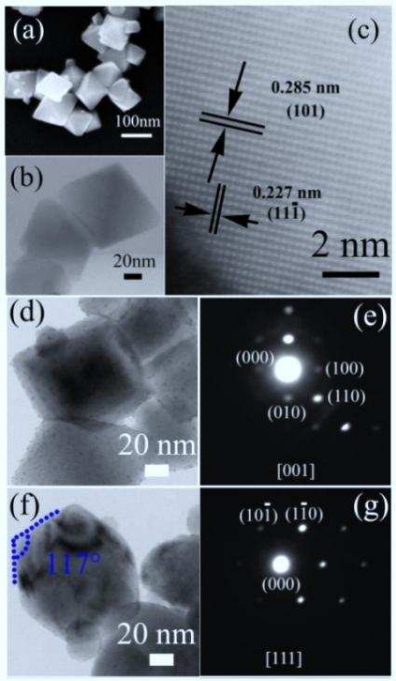

Fig. 2 (a) Typical SEM, (b) TEM and (c) HAADF STEM image of the PT OCT nanocrystals, (d)~(g) TEM images and corresponding electron diffractions of PT OCT nanocrystals along [001] and [111] zone axis, respectively.

Previous researches clearly demonstrated that semiconductors with well-defined facets exposed always result in fascinating optical response, especially in a visible-light range.[10] And these discoveries encourage us to evaluate the degradation ability of the as-synthesized PT OCT nanocrystals under visible-light irradiation. When PT OCT nanocrystals were used as photocatalyst, the photodegradation of MB aqueous solution was completed for 98% after 70 min under visible light irradiation (Fig. S5). As a comparison, we also used $SrTiO_3$ nanoparticles, PT nanofibers with {100} facets exposed [11a] and nanoplates with {001} facets exposed[11b] as photocatalysts to degrade MB aqueous solution. Fig. S6 and S7 present the corresponding XRD patterns and SEM images of the PT nanofibers, nanoplates and $SrTiO_3$ nanoparticles used here. The photodegradation results present in Fig. S8 clearly demonstrated that no obvious photocatalytic activity was observed for these three materials, which further confirms that conventional perovskite oxides are rarely effective visible-light photocatalysts.

Moreover, the reaction rate constant k for blank experiment and P25 in Fig. 3a has been derived from Fig. S5 to be 0.005 and 0.006, respectively. In contrast, the constant k for PT OCT nanocrystals has been determined to be 0.04, very close to that of Bi_2WO_6.[12] This result indicates that PT OCT nanocrystals are highly effective in photodegradation of organic MB pollutants, which has never been achieved in conventional perovskite oxide systems. Furthermore, circle experiments were carried out to identify the stability of PT OCT nanocrystals as photocatalyst, as shown in Fig. 3b. Near 100% degradation of MB at the condition was achieved after 35 min irradiation. Experiencing four circles, PT OCT nanocrystals still demonstrate similar photocatalytic activity as the first circle. As discussed in the emerged oxides such as doped TiO_2[3], $PbBi_2Nb_2O_9$[7] and $BiVO_4$[13], strong absorption of the materials in the range of visible-light wavelength is achieved by intrinsic band structure or designed defect bands within the band gap.

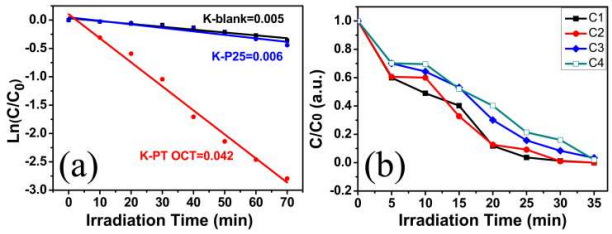

Fig. 3 (a) First-order plots for the photocatalytic degradation of MB using P25 and PT OCT nanocrystals (MB 10^{-5} M and 0.1g catalyst); (b)Cycling tests of visible light-driven photocatalytic activity(MB decomposition) of the PT OCT nanocrystals (MB 1.5×10^{-5} M and 0.6 g catalyst).

To pursue underlying mechanism for the present phenomenon, the optical absorption of the PT OCT nanocrystals was collected to examine the band gap. Fig. 4a shows the absorption spectrum of the as-prepared PT OCT sample, and interestingly, the absorption wavelength of the as-synthesized PT OCT nanocrystals is ~480 nm, corresponding to a band gap of ~2.58 eV. This value is lower than that of the reported PT bulk materials[14], covering a range of visible light. In addition, the optical absorption of PT OCT nanocrystals in the range of 400~700 nm (1.72 eV) was also increased, compared to that of P25. The above results therefore lead us to expect that the visible

ChemComm Accepted Manuscript

This journal is © The Royal Society of Chemistry [year]

light photodegradation performance observed here should be attributed to the change in the band gap of PT OCT nanocrystals. Fig. 4b and 4c shows XPS spectra for Ti 2p and O1s, respectively. The peaks situated at 485.32 eV and 464.14 eV have been identified to be the binding energies of $Ti2p_{3/2}$ and the $Ti2p_{1/2}$ in Fig. 4b, indicative of typical Ti^{4+}. On the other hand, the XPS spectrum for O1s has been well fitted by two peaks at 529.62 eV and 530.91 eV, which is attributed to two kind oxygen ions in tetragonal perovskite PT.[15] As shown in Fig.4d, when the illumination is absent, no signal of magnetic ions or defects can be detected. After illumination, weak ESR signal in the range of 3450~3600 G appeared, which has an origin of Ti^{3+} ions with g= 1.956.[10c] In particular, the localized states within the gap of PT, such as Ti^{3+}, possibly exist, supported by the low-temperature ESR signal of Fig. S9, leading to the unique visible-light absorption in Fig.4a. One should note that PT nanoplates instead of PT OCT nanocrystals can be obtained when the Li ions are absent during the hydrothermal process.[11b] Both of EELS and XPS analysis confirm that there exists a typical Li-O bond on the surface of PT OCT nanocrystals (Fig. S10-S12). The formation of Li-O bond could be greatly beneficial to the surface relaxation and reconstruction and thus the stability of PT OCT nanocrystals, as discussed in F-stabilized {001} TiO_2.[10a] Nevertheless, the electron-hole generation of Li-O excitation under visible light is hardly favorable because of a very high band gap width of 6 ~7.99 eV from O2p to Li1s in most Li-based oxides.[16] Therefore, it is reasonable to consider that Ti-related excitation process probably dominated the optical absorption and the observed photocatalytic activity of PT OCT nanocrystals.

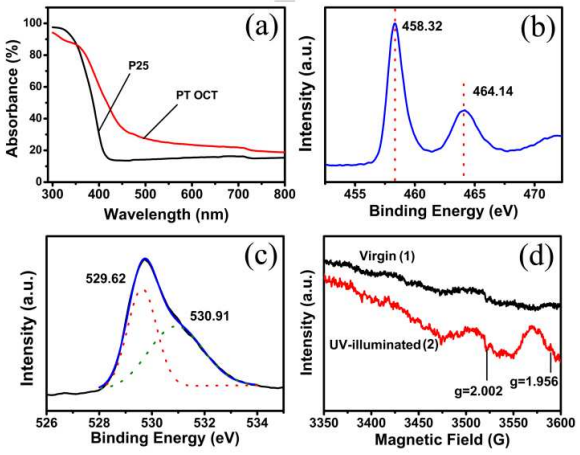

Fig. 4 (a) Spectral absorbance of the PT OCT nanocrystals and P25 TiO_2, XPS spectrum of (b) Ti2p and (c) O1s in PT OCT nanocrystals and (d) ESR spectrum of PT OCT before and after UV-light illumination at ambient temperature.

In conclusion, Li ion-assisted hydrothermal method has been developed to prepare tetragonal perovskite PT OCT nanocrystals, enclosed by {111} facets, where the formation of Li-O bond on the surface of the nanocrystals is essential to the growth and the stability of the OCT nanocrystals. A dramatic high visible-light photocatalytic performance was discovered for PT OCT nanocrystals, and further circle experiments make the PT OCT nanocrystals highly attractive as a new visible-light photocatalyst. It was also revealed that the narrowed optical gap and photocatalytic activity are probably attributed to Ti-related localized states and excitation process, comprehensive understanding of which may trigger more studies on developing novel high-performance visible photocatalyst of perovskite oxides.

We acknowledge the financial support from the National Natural Science Foundation of China (No.51232006, 51102212 and 51102208).

Notes and references

[a] State Key Laboratory of Silicon Materials, Department of Materials Science and Engineering, Cyrus Tang Center for Sensor Materials and Application, Zhejiang University, Hangzhou, P.R.China.
Email: renzh@zju.edu.cn, hgr@zju.edu.cn
[b] EMAT, University of Antwerp, Groenenborgerlaan 171, B-2020 Antwerp, Belgium
[c] Electron Micriscope Center of Zhejiang University, Hangzhou, 310027, P.R. China

† Electronic supplementary information (ESI) available: Detailed experiments and characterization. See DOI: 10.1039/b000000x/
‡These authors contributed equally to this work.

1 A. Kudo, Y. Miseki, *Chem. Soc. Rev.*, 2009, **38**, 253-278.
2 (a) A. Fujishima, K. Honda, *Nature*, 1972, **238**, 37-38; (b) K. Hashimoto, H. Irie and A. Fujishima, *Jpn. J. Appl. Phys.*, 2005, **44**, 8269-8285.
3 (a) R. Asahi, T. Morikawa, T. Ohwaki, K. Aoki and Y. Taga, *Science*, 2001, **293**, 269-271. (b) S. In, A. Orlov, R. Berg, F. Garcia, S. Pedrosa-Jimenez, M. S. Tikhov, D. S. Wright and R. M. Lambert, *J. Am. Chem. Soc.*, 2007, **129**, 13790-13791. (c) X. B. Chen, L. Liu, P. Y. Yu and S. S. Mao, *Science,* 2011, **331**, 746-750.
4 F. E. Osterloh, *Chem. Mater.*, 2008, **20**, 35-54.
5 (a) H. Mizoguchi, K. Ueda, M. Orita, S. C. Moon, K. Kajihara, M. Hirano and H. Hosono, *Mater. Res. Bull.*, 2002, **37**, 2401-2406. (b) X. Wei, G. Xu, Z. H. Ren, C. X. Xu, W. J. Weng, G. Shen and G. R. Han, *J. Am. Ceram. Soc.*, 2010, **93**, 1297-1305. (c) F. Gao, X. Y. Chen, K. B. Yin, S. Dong, Z. F. Ren, F. Yuan, T. Yu, Z. G. Zou and J. M. Liu, *Adv. Mater.*, 2007, **19**, 2889-2892. (d) S. Li, Y. H. Lin, B. P. Zhang, Y. Wang and C. W. Nan, *J. Phys. Chem. C*, 2010, **114**, 2903-2908.
6 (a) J. H. Luo, P. A. Maggard, *Adv. Mater.*, 2006, **18**, 514-517. (b) S. Li, Y. H. Lin, B. P. Zhang, J. F. Li and C. W. Nan, *J. Appl. Phys.*, 2009, **105**, 054310. (c) F. Zou, Z. Jiang, X. Q. Qin, Y. X. Zhao, L. Y. Jiang, J. F. Zhi, T. C. Xiao and P. P. Edwards, *Chem. Comm.*, 2012, **48**, 8514-8516.
7 H. G. Kim, D. W. Hwang and J. S. Lee, *J. Am. Chem. Soc.*, 2004, **126**, 8912-8913.
8 A. M. Glazer, S. A. Mabud, *Acta Cryst.*, 1978, **B34**, 1065-1067.
9 Y. F. Hao, G. W. Meng, C. H. Ye and L. D. Zhang, *Cryst. Growth Des.*, 2005, **5**, 1617-1621.
10 (a) H. G. Yang, C. H. Sun, S. Z. Qiao, J. Zou, G. Liu, S. C. Smith, H. M. Cheng and G. Q. Lu, *Nature*, 2008, **453**, 638-641. (b) G. Liu, J. C. Yu, G. Q. Lu and H. M. Cheng, *Chem. Commun.*, 2011, 47, 6763-6783. (c) Z. Zhao, H. Q. Tan, H. F. Zhao, Y. Lv, L. J. Zhou, Y. J. Song and Z. C. Sun, *Chem. Commun.*, 2014, DOI: 10.1039/C3CC49182J.
11 (a) Z. Y. Liu, Z. H. Ren, Z. Xiao, C. Y. Chao, X. Wei, Y. Liu, X. Li, G. Xu, G. Shen, G. R. Han, *Small*, 2012, **8**, 2959-2963. (b) C. Y. Chao, Z. H. Ren, Y. H. Zhu, Z. Xiao, Z. Y. Liu, G. Xu, J. Q. Mai, X. Li, G. Shen and G. R. Han, *Angew. Chem. Int. Ed.*, 2012, **51**, 9283-9287.
12 C. Zhang and Y. F. Zhu, *Chem. Mater.*, 2005, **17**, 3537-3545.
13 A. Kudo, K. Ueda, H. Kato and I. Mikami, *Catal. Lett.*, 1998, **53**, 229-230.
14 S. Piskunov, E. Heifets, R. I. Eglitis and G. Borstel, *Comp. Mater. Sci.*, 2004, **29**, 165-178.
15 H. S. Gu, Y. M. Hu, J. You, Z. L. Hu, Y. Yuan and T. J. Zhang, *J. Appl. Phys.*, 2007, **101**, 024319.
16 V. V. Maslyuk, *Phys. Rev. B*, 2005, **72**, 125101.

ChemComm Accepted Manuscript

Graphical Abstract

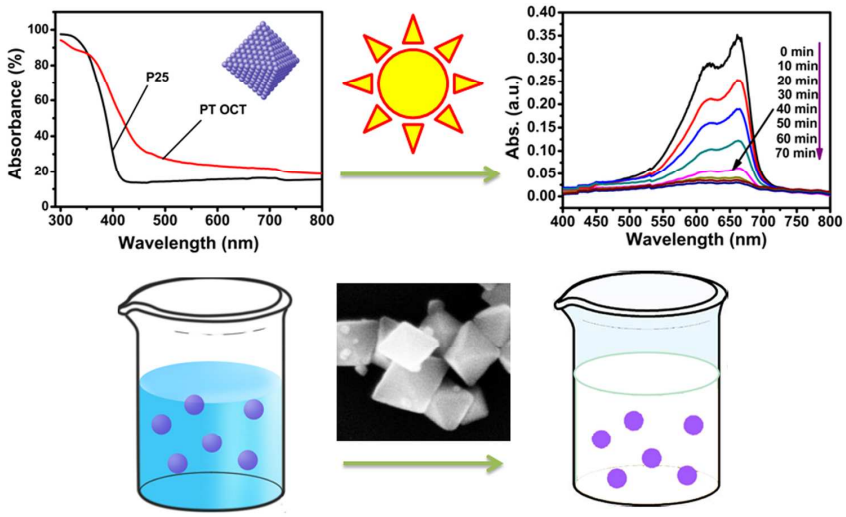

Octahedral-shaped perovskite $PbTiO_3$ nanocrystals have been successfully synthesized for the first time via a facile hydrothermal method by the introduction of lithium nitride. Further photocatalytic degradation of MB aqueous solution proves that these perovskite octahedrons possess effective photocatalytic activity under visible light irradiation, which would certainly provide incentives for more studies to develop visible light photocatalyst among perovskite family.

ChemComm Accepted Manuscript